UCLA
COMPUTATIONAL AND APPLIED MATHEMATICS

Flow Under Geodesic Curvature

David L. Chopp

May 1992

CAM Report 92-23

Department of Mathematics
University of California, Los Angeles
Los Angeles, CA. 90024-1555

Flow Under Geodesic Curvature

David L. Chopp *
Mathematics Department
University of California
Los Angeles, California 90024

May 20, 1992

Abstract

In this paper, the equations of motion for curves flowing with curvature dependent speed in 2-dimensional Euclidean space, are extended to geodesic curvature flow on 2-dimensional manifolds. The equations of motion are based on a technique of locally embedding a curve γ on a manifold M as a level set of a function $\phi : M \to R$. The velocity of γ is computed on fixed coordinate patches of M. Several examples of manifolds and initial curves are computed.

1 Introduction

In this paper, the flow of curves on two-dimensional manifolds moving with speed dependent on the geodesic curvature is studied. The equations of motion are a generalization of the Euclidean version introduced by Osher and Sethian in [3]. In this context, a curve is locally represented as a level set of a real valued function defined on the manifold.

All computing is done on simply connected coordinate patches of the manifold projected into R^2. By restricting the level set function ϕ to coordinate patches, it is possible to study single curves on non-simply connected manifolds (e.g. a torus). The function ϕ is constructed on each local patch so that the flow in overlap regions between patches is consistent.

Similar to the minimal surface calculations by the author and Sethian in [1, 2], boundary conditions can be added to the motion of the curve. In this case, if the curve moves with speed equal to the geodesic curvature, a curve with fixed endpoints would flow towards a geodesic of the manifold (i.e. a curve with constant geodesic curvature zero).

*Supported by the National Science Foundation under grant CTS-9021021.

2 Equations of Motion

Consider a 2-dimensional manifold $M \subset R^3$. Let $\gamma(t) \subset M$, for $t \in [0, \infty)$, be a family of closed curves moving with speed $F(\kappa_g)$ in the direction normal to itself on M. Here, κ_g is the geodesic curvature of $\gamma(t)$ on M. Let $g_t(s)$ be the parameterization of $\gamma(t)$ by arc length.

First assume that M is orientable. In this case, the unit normal map N is continuous on M. At every point $g_t(s)$, a natural coordinate system for T_M is given by the vectors $g_t'(s)$, $N \times g_t'(s)$. Thus, for any point $x(t) \in \gamma(t)$, the velocity under this flow is given by

$$\dot{x} \cdot (N \times g_t') = F(\kappa_g).$$

Following a derivation in [5], the expression for geodesic curvature is

$$\kappa_g = (N \times g_t') \cdot g_t''. \tag{1}$$

Note that a change in sign of the unit normal N results in a corresponding change in sign of κ_g. If F is an odd function, then $\dot{x}$ is independent of the choice of N. However, if F is not an odd function, then the choice of the normal changes the flow. Therefore, if M is not orientable, then only odd speed functions F are allowed. The algorithm presented here also requires that F be an odd function when M is not simply connected.

2.1 Level Set Representation

It was demonstrated in [4], that using a marker particle method to model curvature flow can lead to instability during computation. For that reason, an alternative representation of a curve in R^2 was given in [3]. In this context, given a curve $\gamma(t)$ on M we define a real valued function $\phi(x, t)$ such that $\phi^{-1}(0, t) = \gamma(t)$. Each level set of ϕ becomes a different initial curve moving with the same speed function. The equation of motion is then rewritten as an evolution equation for ϕ.

As noted in [3], the level set representation enables the flow to change topology naturally, without stability problems or *ad hoc* user intervention.

2.2 Generalized Equations of Motion

Assume the manifold M is given by $M = f^{-1}(0)$, where $f : R^3 \to R$. We break the manifold into a collection of coordinate maps, $\{(U_i, \pi_i)\}$ such that $M = \cup U_i$, each set U_i is simply connected, and $\pi_i : U_i \to V_i \subset R^2$ is a bijection.

The computing is done on the collection of sets $V_i = \pi_i(U_i)$. We define the function $\Phi_i : V_i \to R$ by $\Phi_i(x, t) = \phi(\pi_i^{-1}(x), t)$, so that $\phi(x, t)|_{U_i} = \Phi_i(\pi_i(x), t)$.

In order to write the equations of motion in the level set representation, we must compute a velocity field on the entire manifold M. We compute the

velocity field on each coordinate patch and then see that it is consistent in regions of overlap. For this section, assume $\phi = \phi|_{U_i}$. At any point $x \in U_i$, the velocity vector will be normal to the level set of ϕ containing x, in the tangent space $T_M(x)$, and have length $F(\kappa_g)$.

First, we compute the geodesic curvature of the curve $\phi^{-1}(C)$ in terms of ϕ, and then in terms of the Φ_i. Assume the set $\phi^{-1}(C)$ is given by the curve $g(s)$ parameterized by arc length. According to equation (1), to compute κ_g we need the normal to M, and the velocity and acceleration vectors for $g(s)$. The unit normal N to M is given by $N = \nabla f/\|\nabla f\|$. Since $g(s)$ is parameterized by arc length, we have $\|g'(s)\| = 1$, $g'(s) \perp \nabla\phi$, and $g'(s) \perp \nabla f$. Thus, the velocity vector τ of $g(s)$ is given by

$$\tau = g'(s) = \frac{\nabla f \times \nabla \phi}{\|\nabla f \times \nabla \phi\|}.$$

The choice of τ is not arbitrary, but is chosen with respect to the unit normal of the curve in T_M so that the sign of the geodesic curvature agrees witht the usual formula for curvature in the plane. We also have $g''(s) \perp g'(s)$, so

$$g''(s) = \alpha\nabla\phi + \beta\nabla f \tag{2}$$

for some values α and β. Furthermore, recall that $\phi(g(s)) = C$ and $f(g(s)) = 0$ for all s. Differentiating twice with respect to s, we get

$$\tau \cdot (\nabla^2\phi \cdot \tau) + \nabla\phi \cdot g''(s) = 0 \tag{3}$$
$$\tau \cdot (\nabla^2 f \cdot \tau) + \nabla f \cdot g''(s) = 0 \tag{4}$$

Substituting equation (2) into equations (3), (4) and solving for α, we get

$$\alpha = \frac{\tau \cdot \left[((\nabla\phi \cdot \nabla f)\nabla^2 f - (\nabla f \cdot \nabla f)\nabla^2\phi) \cdot \tau\right]}{(\nabla\phi \cdot \nabla\phi)(\nabla f \cdot \nabla f) - (\nabla\phi \cdot \nabla f)^2}$$

Therefore, the geodesic curvature κ_g is given by

$$\begin{aligned}
\kappa_g &= g'' \cdot [N \times g'] \\
&= (\alpha\nabla\phi + \beta\nabla f) \cdot [N \times \tau] \\
&= \alpha\nabla\phi \cdot [N \times \tau] \\
&= \frac{[N \times \tau] \cdot n}{1 - (n \cdot N)^2} \left\{ \tau \cdot \left[\left(\frac{n \cdot N}{\|\nabla f\|}\nabla^2 f - \frac{1}{\|\nabla\phi\|}\nabla^2\phi \right) \cdot \tau \right] \right\}
\end{aligned}$$

where $n = \nabla\phi/\|\nabla\phi\|$ and $N = \nabla f/\|\nabla f\|$.

Next, we compute the direction of the velocity vector v. The direction of the velocity vector is the same as the orthogonal projection of $\nabla\phi$ onto T_M. Therefore,

$$v = \tau \times N = \frac{n - (n \cdot N)N}{\|n - (n \cdot N)N\|}$$

and the velocity at x on M is described by

$$\dot{x} \cdot v = F(\kappa_g).$$

The computing is done on the images of the coordinate patches $\pi_i(U_i)$, so the velocity must be translated into the velocity for points on the coordinate patches. Recall that $\phi(x,t)|_{U_i} = \Phi_i(\pi_i(x),t)$, hence we replace $\nabla\phi$ with $\nabla\Phi_i \circ D\pi_i$ and $\nabla^2\phi$ with $(D\pi_i)^t \circ \nabla^2\Phi_i \circ D\pi_i + \nabla\Phi_i \circ D^2\pi_i$ according to the chain rule. The map $D\pi_i : T_M \to T_{R^2}$ maps the velocity field given on M to the velocity field on $\pi_i(U_i)$. Therefore, for a point $x \in \pi_i(U_i)$, the equation of motion is described by

$$\dot{x} \cdot \eta = F(\kappa_g) D\pi_i(v) \cdot \eta$$

where $\eta = \nabla\Phi_i / \|\nabla\Phi_i\|$ is the unit normal to the level set containing $\Phi_i(x)$.

Let

$$\tilde{F}(\kappa_g) = F(\kappa_g) D\pi_i(v) \cdot \nabla\Phi_i / \|\nabla\Phi_i\|. \tag{5}$$

Assume $\Phi_i(x(t),t) = C$, then differentiating with respect to t gives

$$\begin{aligned} 0 &= \Phi_{it} + \nabla\Phi_i \cdot \dot{x} \\ &= \Phi_{it} + \|\nabla\Phi_i\| \left(\frac{\nabla\Phi_i}{\|\nabla\Phi_i\|} \right) \cdot \dot{x} \\ &= \Phi_{it} + \tilde{F}(\kappa_g) \|\nabla\Phi_i\|. \end{aligned} \tag{6}$$

3 Numerical Method

The general algorithm can be stated as follows:

1. Choose coordinate patches and maps to represent the manifold M.
2. Initialize the functions Φ_i on each coordinate patch.
3. Compute the boundary values in each coordinate patch based upon overlap values with neighboring patches.
4. Advance each Φ_i in time according to the differential equation (6).
5. Go to step 3.

At any time t, the curve $\gamma(t)$ can be reconstructed from

$$\gamma(t) = \cup \pi_i^{-1}(\Phi_i^{-1}(0,t)) \tag{7}$$

We will now discuss the details of each of these steps.

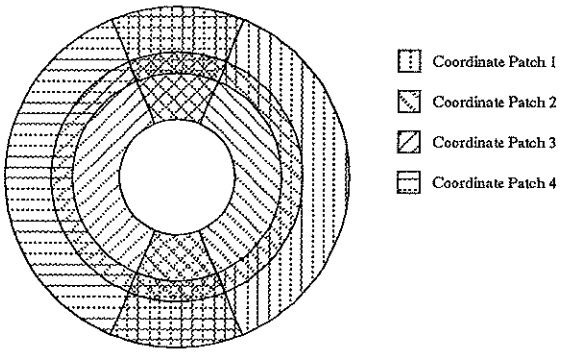

Figure 1: Example of coordinate patches on a torus.

3.1 Constructing the Grid

Given a manifold M the collection of coordinate patches $\{(U_i, \pi_i)\}$ must be chosen. Define $V_i = \pi_i(U_i)$. It is important to choose simply connected coordinate patches, so that any simple curve can be represented by a level set of a function ϕ on U_i. The equations given above are for the case when π_i maps onto a rectangular coordinate system in R^2.

In the overlap sets, where $U_i \cap U_j \neq \emptyset$, there must be at least a three grid point overlap between the sets V_i and V_j. Computing the boundary conditions for each V_i is made easier if the grid points and projection maps π_i are chosen so that if $x \in V_i$ is a grid point in V_i and $\pi_i^{-1}(x) \in U_i \cap U_j$, then $\pi_j(\pi_i^{-1}(x))$ is also a grid point in V_j.

For example, let M be a torus with large radius R and small radius r symmetric about the z-axis. One choice of coordinate patches is

$$\begin{aligned} U_1 &= \left\{(x,y,z) : \sqrt{x^2+y^2} > R-\epsilon, x > -\epsilon\right\} \\ U_2 &= \left\{(x,y,z) : \sqrt{x^2+y^2} < R+\epsilon, x > -\epsilon\right\} \\ U_3 &= \left\{(x,y,z) : \sqrt{x^2+y^2} < R-\epsilon, x < \epsilon\right\} \\ U_4 &= \left\{(x,y,z) : \sqrt{x^2+y^2} > R-\epsilon, x < \epsilon\right\} \end{aligned}$$

where each $\pi_i : U_i \to V_i = (-\pi/2 - \epsilon, \pi/2 + \epsilon) \times (-\pi/2 - \epsilon, \pi/2 + \epsilon)$ in the natural way. Then a uniform rectangular grid is placed on the closure of V_i. A diagram of this choice of coordinate maps is given in figure 1. Notice that the grid points at the edges of each coordinate patch match up in the overlap regions.

3.2 Initialization of Φ_i

The objective when initializing the functions Φ_i is to satisfy equation (7). One way to do this is to use the signed distance function. For each grid point $x \in V_i$, compute $\text{dist}(\pi_i^{-1}(x), \gamma)$, where $\text{dist}(x, y)$ is the distance between x and y in the space M is embedded. Then on each V_i, choose a reference grid point y which has non-zero distance and assign $\Phi_i(y)$ to be positive. For the remaining grid points, the sign of $\Phi_i(x)$ is determined by the number of times a line segment connecting x and y crosses the set $\pi_i(\gamma)$, with $\Phi_i(x) < 0$ for an odd number and $\Phi_i(x) > 0$ for an even number.

By using the distance function in the manifold space, this ensures that at each grid point $x \in U_i \cap U_j$,

$$|\Phi_i(\pi_i(x))| = |\Phi_j(\pi_j(x))|.$$

This is important because locally, for each i such that $x \in U_i$, we must have

$$\phi(x) = \pm\Phi_i(\pi_i(x))$$

to preserve consistent motion in the overlap regions.

Recall that a consistent choice of normals for both the manifold and the curve γ is necessary when F is not an odd function. Therefore, if F is not an odd function, we must additionally require $\phi(x) = \Phi_i(\pi_i(x))$ in order to maintain a consistent velocity field.

3.3 Connecting Multiple Patches

The motion by curvature on each patch is computed on the interior grid points of each patch V_i. The values at the boundary are taken from neighboring patches. Let x be a grid point on the boundary of V_i. By construction, $\pi_i^{-1}(x)$ is in the interior of some other patch U_j. Therefore, we have $\Phi_i(x) = \pm\Phi_j(\pi_j(\pi_i^{-1}(x)))$, where the sign is determined by whether $\Phi_i \circ \pi_i$ and $\Phi_j \circ \pi_j$ are of equal (plus) or opposite (minus) sign in the interior of the region $U_i \cap U_j$.

Two coordinate patches may have two or more disconnected overlap regions on M. The sign convention must be determined individually for each distinct overlap. For example, the two outer patches on the torus example below overlap in two distinct locations. It is possible for both patches to share the same sign convention in one overlap while having the opposite convention in the other overlap. This property makes it possible to model any single curve on a torus as a level set of a function within each coordinate patch.

3.4 Calculation on a Single Patch

Following the argument in [3], we break the function F into the constant and non-constant parts, $\tilde{F}(\kappa) = \tilde{F}_1 - \tilde{F}_2(\kappa)$. Equation (6) then becomes,

$$\Phi_{it} + \tilde{F}_1\|\nabla\Phi_i\| = \tilde{F}_2(\kappa_g)\|\nabla\Phi_i\| \tag{8}$$

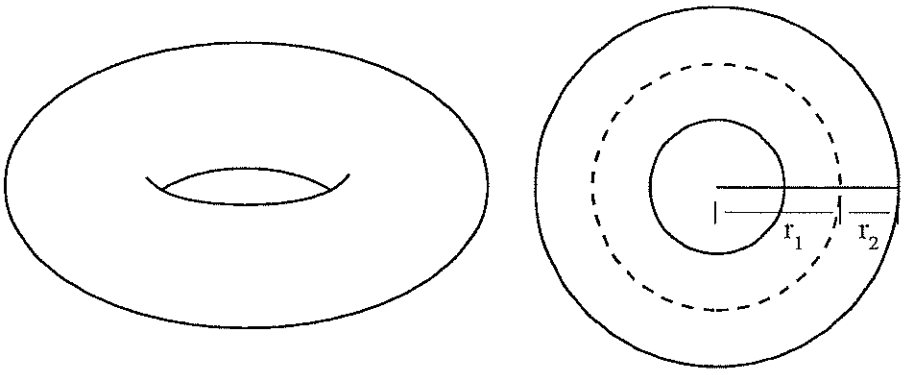

Figure 2: Torus Diagram

This equation can be viewed as a Hamilton-Jacobi like equation with parabolic right hand side. Upwind techniques from hyperbolic conservation laws are used to compute the left hand side and central differences are used on the right hand side.

4 Examples

4.1 Example Manifold Construction

To illustrate the algorithm, we will construct a representation of a torus and flow an initial curve on the torus. First, the torus will be described as the zero level set of $f(x,y,z) = z^2 + (r_1 - \sqrt{x^2+y^2})^2 - r_2^2$ (see figure 2). Let each patch map onto the rectangular region $V = [-1-\epsilon_x, 1+\epsilon_x] \times [-1-\epsilon_y, 1+\epsilon_y]$ with $M \times N$ grid points. Define $\Delta x = 2/(M-2)$, $\Delta y = 2/(N-2)$, $\epsilon_x = \Delta x$, and $\epsilon_y = \Delta y$. Next, define

$$\begin{aligned}
\pi_1^{-1}(x,y) &= ((r_1 + r_2\cos(\pi y/2))\cos(\pi x/2), (r_1 + r_2\cos(\pi y/2))\sin(\pi x/2), \\
&\quad r_2\sin(\pi y/2)) \\
\pi_2^{-1}(x,y) &= ((r_1 - r_2\cos(\pi y/2))\cos(\pi x/2), (r_1 - r_2\cos(\pi y/2))\sin(\pi x/2), \\
&\quad r_2\sin(\pi y/2)) \\
\pi_3^{-1}(x,y) &= (-(r_1 - r_2\cos(\pi y/2))\cos(\pi x/2), (r_1 - r_2\cos(\pi y/2))\sin(\pi x/2), \\
&\quad r_2\sin(\pi y/2)) \\
\pi_4^{-1}(x,y) &= (-(r_1 + r_2\cos(\pi y/2))\cos(\pi x/2), (r_1 + r_2\cos(\pi y/2))\sin(\pi x/2), \\
&\quad r_2\sin(\pi y/2)).
\end{aligned}$$

Finally, the patches on the torus are defined by $U_i = \pi_i^{-1}(V)$ and $\pi_i = (\pi_i^{-1})^{-1}$. See figure 3 for a picture of how the patches and grid points fit together.

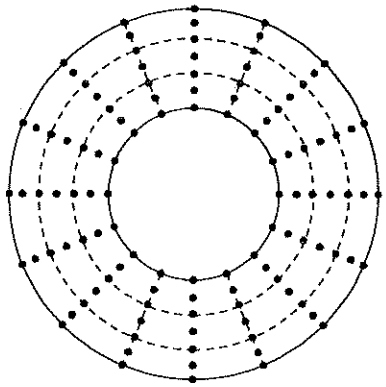

Figure 3: Patches and grid points on the torus

To demonstrate the initialization process, we begin with a simple loop given by

$$\gamma(s) = (r_1 + r_2\cos(s), 0, r_1 + r_2\sin(s)).$$

The curve passes through patches 1 and 2, but not patches 3 and 4. Note that a single scalar function could not have $\gamma(s)$ as its zero-level set on the torus because an additional sign change is necessary somewhere else. However, by using local patches, it is possible to hide the necessary sign change in the overlap regions.

After the positive distance from each point on the torus to γ is computed (i.e. $|\Phi_i(x,y)|$ is determined for all i, x, and y), the sign at each point must be chosen. On V_1 and V_2, choose $\Phi_i(x,y) < 0$ for $x < 0$. On V_3 and V_4, choose $\Phi_i(x,y) > 0$.

Finally, we describe how to set the boundary values for V_1. Let the grid be represented by the points $x_{i,j}$. The points $x_{1,j}$ for $j = 2,\ldots,N-1$ are determined by the overlap between U_1 and U_4. The sign σ in the overlap is given by

$$\sigma = \Phi_1(x_{2,j})/\Phi_4(\pi_4(\pi_1^{-1}(x_{2,j}))).$$

In this example, $\sigma = -1$. Therefore,

$$\Phi_1(x_{1,j}) = -\Phi_4(\pi_4(\pi_1^{-1}(x_{1,j}))).$$

On the other hand, the points $x_{M,j}$ for $j = 2,\ldots,N-1$ are also determined by the overlap between U_1 and U_4, but for these points $\sigma = +1$. Therefore,

$$\Phi_1(x_{M,j}) = \Phi_4(\pi_4(\pi_1^{-1}(x_{M,j}))).$$

Similarly, $\Phi_1(x_{i,1})$ and $\Phi_1(x_{i,N})$ are determined by the overlap between U_1 and U_2. Finally, $\Phi_1(x_{1,1})$, $\Phi_1(x_{M,1})$, $\Phi_1(x_{1,N})$, and $\Phi_1(x_{M,N})$ are determined by

the overlap between U_1 and U_3. The boundaries for the other patches are determined accordingly.

In order to have a consistent flow in the overlap regions, it is necessary for the speed function F to be an odd function. As noted earlier, this allows for the flow to be independent of the normal to the level set. Thus, even though $\Phi_1 \circ \pi_1$ and $\Phi_4 \circ \pi_4$ have opposite sign in the region $U_1 \cap U_4$, the flow is the same because the motion of the level sets is independent of the choice of sign (which determines the normal to the level set). This means that we should have $|\Phi_1 \circ \pi_1(x)| = |\Phi_4 \circ \pi_4(x)|$ for all time in the overlap region.

Surfaces which are simply connected do not have the restriction that F be odd because it is possible to ensure that even the signs agree in the overlap regions. However, in the level set representation it is possible to guarantee consistent flow in the overlap regions only when F is odd or the manifold is simply connected.

4.2 Sample Computations

We begin with flow on a sphere. The sphere is constructed with a single coordinate patch with the projection mapping the sphere onto its spherical coordinate system, the square $[-\pi, \pi] \times [-\pi, \pi]$. The gap in figures 4 and 5 shows the boundary of the coordinate patch. Figure 4 shows an initial circle just smaller than a great circle shrinking to a point at the top. Figure 5 shows a periodic curve symmetric with respect to the equator collapsing to the equator.

Next, we show flow on a torus. If the torus is constructed with a single coordinate patch, then it is not possible to model a single non-contractible curve using a level set approach. For curves which are not too complicated, it is possible to construct a second curve to allow for the level set formulation. In figure 6, a single coordinate patch is used and the flow of two non-intersecting curves is computed.

However, if multiple coordinate patches are used, then a required sign change can be handled by the communications between coordinate patches. Therefore, it is possible to model a single curve on a torus. Figure 7 shows a single curve flowing on a torus. The coordinate patches for the torus are described in section 4.1.

Subsets of manifolds can also be used. For example, we compute the flow of an oval and a periodic curve on a helicoid. The boundary conditions are periodic at the top and bottom, one sided derivatives on the sides of a single rectangular coordinate patch. Figure 8 shows the oval as it shrinks to a point, while figure 9 shows the periodic curve flowing towards the central axis of the helicoid.

Another example of flow on a submanifold is when the manifold is the graph of a function $f : R^2 \rightarrow R$. In this example, we use $f(x, y) = 2\cos(2\sqrt{x^2 + y^2})$. One-sided derivatives are used for all boundaries of a rectangular region of this

graph. Figure 10 shows a straight line perturbed off-center flowing away from the center over a ridge.

Finally, we show several flows on a cube. The cube is constructed with six coordinate patches corresponding to the faces of the cube. The first experiment on the cube involves a comparing the flow on a cube with orthogonal edges to the flow on a cube with constructed round edges. Figures 11–14 show the orthogonal cube followed by three different rounded cubes with the same initial curve. The initial curve is flatter on the front faces than on the top. We see that the flow is similar in all cases with the curve collapsing to a point near the corner. Two other flows on a cube are shown in figures 15 and 16.

References

[1] D. L. Chopp. Computing minimal surfaces via level set curvature flow. Technical Report LBL-30685, Lawrence Berkeley Laboratory, May 1991.

[2] D. L. Chopp and J. A. Sethian. Flow under mean curvature: Singularity formation and minimal surfaces. Technical Report PAM-541, Center for Pure and Applied Mathematics, University of California, Berkeley, November 1991.

[3] S. Osher and J. Sethian. Fronts propagating with curvature-dependent speed: Algorithms based on Hamilton-Jacobi formulations. *Journal of Computational Physics*, 79(1), November 1988.

[4] J. Sethian. A review of recent numerical algorithms for hypersurfaces moving with curvature-dependent speed. *Journal of Differential Geometry*, 31:131–161, 1989.

[5] T. J. Willmore. *An Introduction to Differential Geometry*. Oxford University Press, 1959.

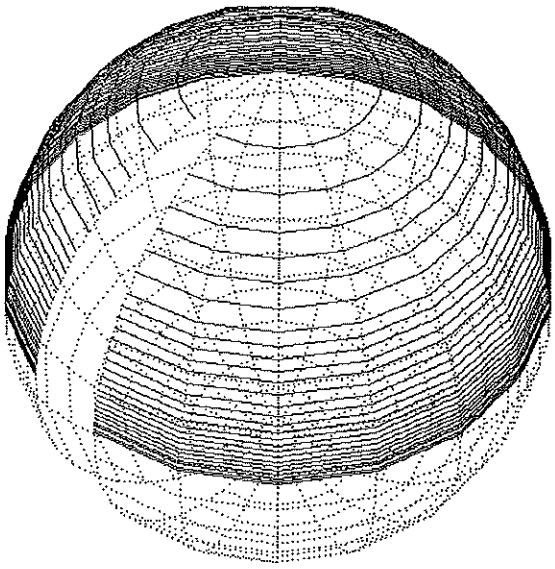

Figure 4: Circle shrinking on a sphere

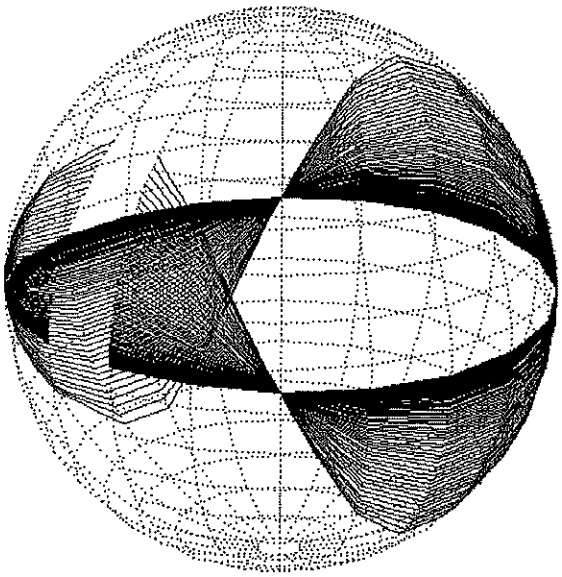

Figure 5: Periodic curve shrinking to a great circle

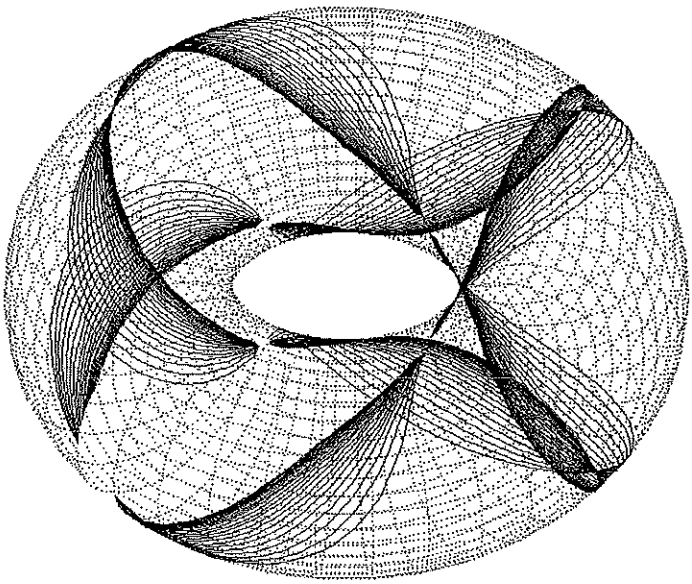

Figure 6: Two curves flowing on a torus

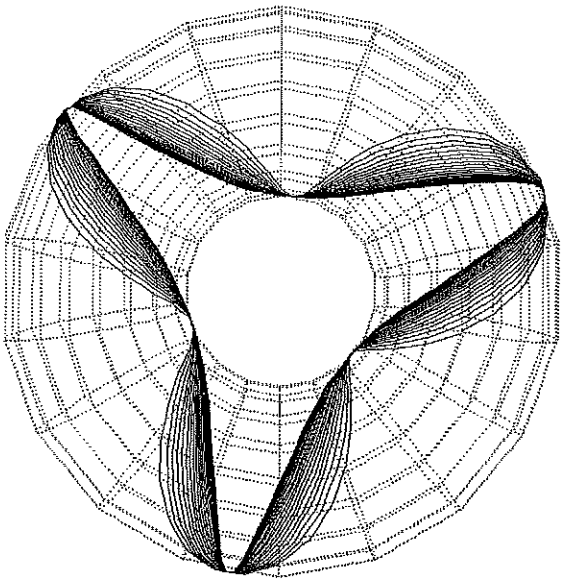

Figure 7: A single curve flowing on a torus

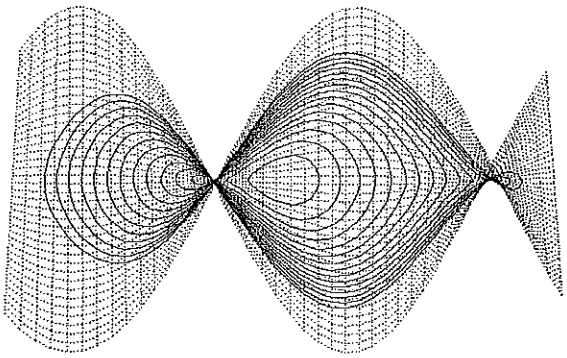

Figure 8: A single loop shrinking on a helicoid

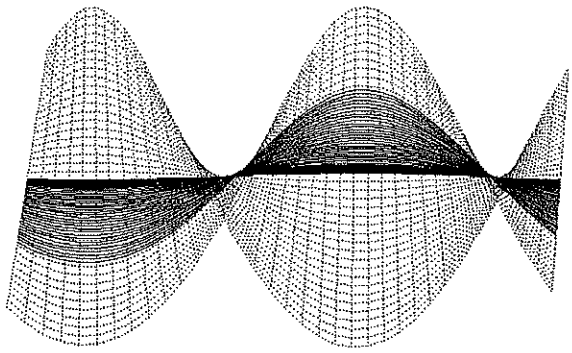

Figure 9: A periodic curve on a helicoid

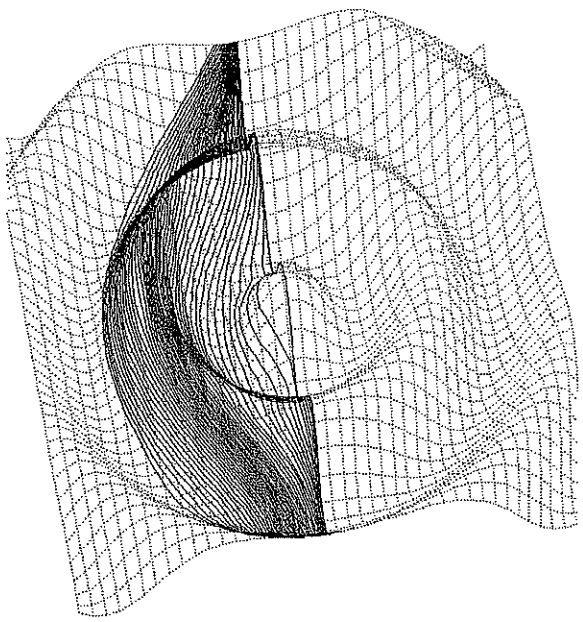

Figure 10: A curve flowing on the graph of $f(x, y) = 2\cos(2\sqrt{x^2 + y^2})$

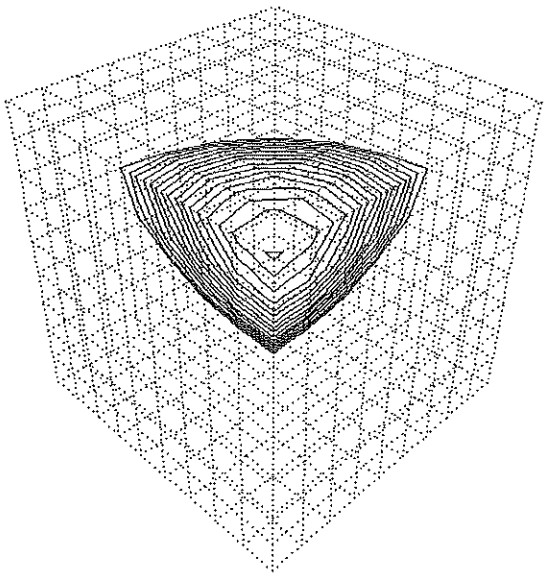

Figure 11: A single loop flowing on a cube with orthogonal edges

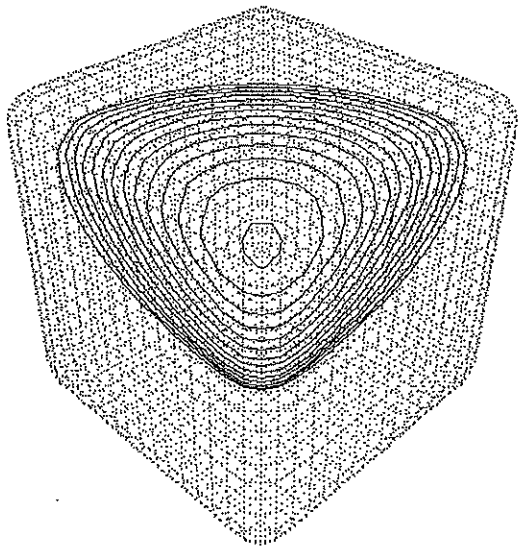

Figure 12: A single loop flowing on a cube with large rounded edges

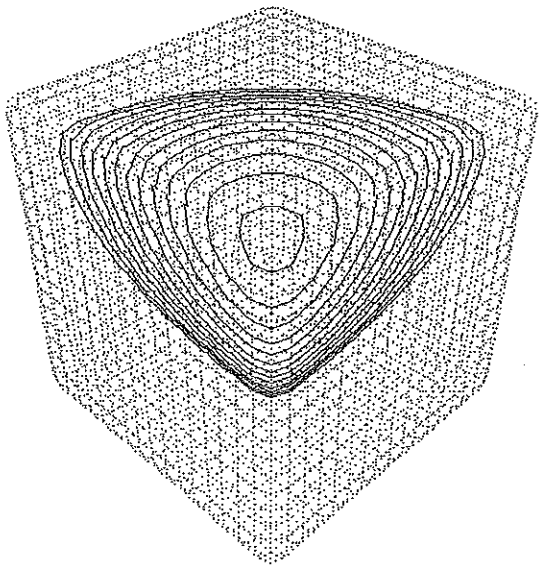

Figure 13: A single loop flowing on a cube with medium rounded edges

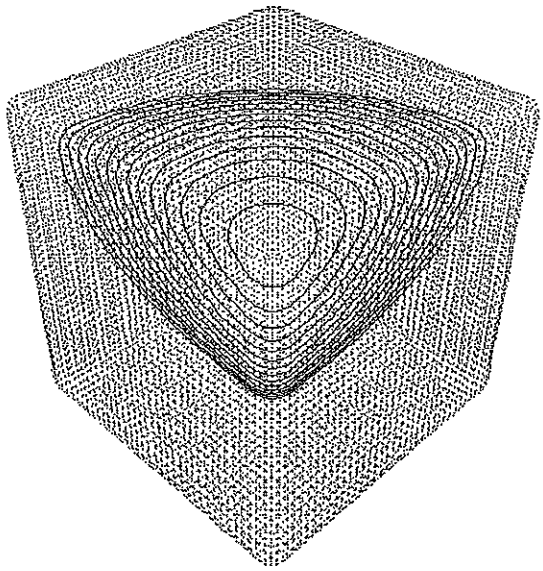

Figure 14: A single loop flowing on a cube with small rounded edges

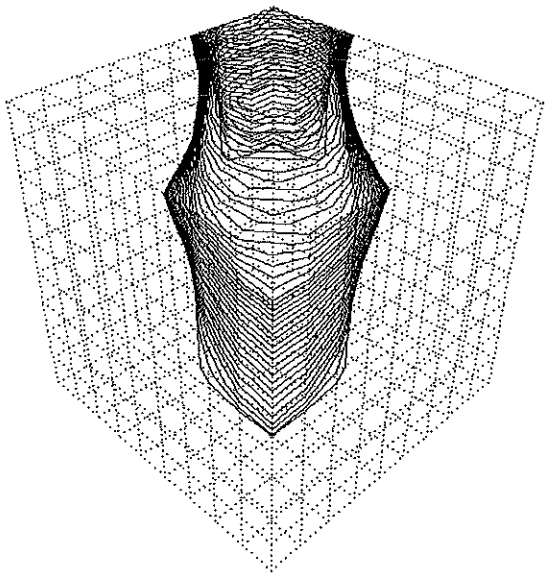

Figure 15: A single loop pulled over two opposite corners on a face

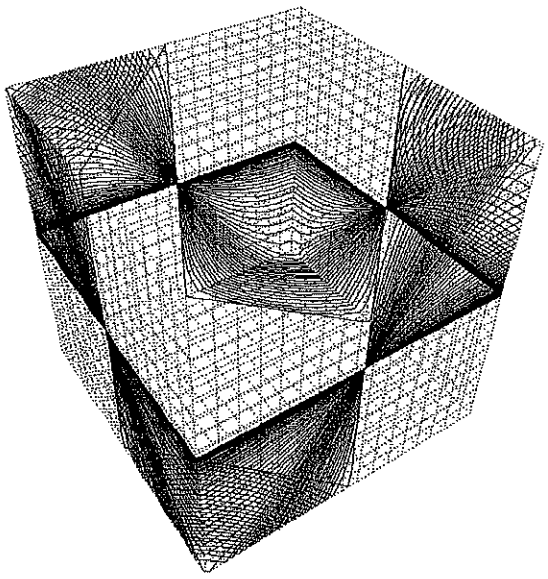

Figure 16: A single loop pulled over alternating corners